Biogenic synthesis of silver nanoparticles from leaf extract of *Elettaria cardamomum* and their antifungal activity against phytopathogens

Pragati Jamdagni, Poonam Khatri, J. S. Rana*

Department of Biotechnology, Deenbandhu Chhotu Ram University of Science and Technology, Murthal 131039, Sonipat, Haryana, India

*Corresponding author

DOI: 10.5185/amp.2018/977
www.vbripress.com/amp

Abstract

The current study reports biogenic synthesis of silver nanoparticles from *Elettaria cardamomum*. *Elettaria* leaf extract was used as reducing and capping agent for nanoparticle synthesis from parent solution of silver nitrate. Nanoparticle suspension was characterized mainly using UV-Visible spectroscopy. Synthesis parameters namely, time, metal ion concentration, leaf extract quantity, reaction temperature and pH are well known to affect the final product of synthesis and hence, were varied to assess optimum conditions for synthesis. Nanoparticles synthesized at optimum conditions were washed and characterized using Fourier Transform Infrared Spectroscopy (FTIR), X-ray diffraction (XRD), Dynamic Light Scattering (DLS) and Transmission Electron Microscopy (TEM). Nanoparticles obtained were in the size range of 5-80 nm (TEM), with an average particle size of 29.96 nm as calculated using Debye-Scherrer formula and average hydrodynamic diameter of 32.12 nm (DLS). FTIR implicates plausible role of protein part of leaf extract in nanoparticle synthesis and DLS confirms monodisperse nature of the suspension. Nanoparticle suspension was found to be stable after four months of storage at room temperature without the addition of any stabilizing agents. Silver nanoparticles exhibited excellent antifungal activity against various fungal phytopathogens with minimum inhibitory concentration as low as 8 µg/mL for *Aspergillus niger*, making them potential antifungal agents in the field of agriculture.

Keywords: Silver nanoparticles, *elettaria cardamomum*, optimization, characterization, antifungal activity.

Introduction

Nobel laureate Richard Feynman delivered a lecture entitled 'There's Plenty of Room at the Bottom' at California Institute of Technology in the year 1959 and laid the foundation of a new exciting field of science **[1]**. Since its inception, nanotechnology has fascinated research fraternity all over the world owing to extremely different and unique physical and chemical properties exhibited by nanostructures as compared to their bulk equivalents **[2]**. Nanoparticles are one among various nanostructures and are finding applications in nearly every possible field of our day-to-day lives **[3-9]**. Basic approaches primarily followed for nanoparticle synthesis are top down and bottom up approaches. Top down approaches are "break down" technologies and employ mechanical and physical processes such as laser ablation, atomization etc. Bottom up approaches are "build up" technologies that are based upon chemical principles and follow methods such as pyrolysis, sol-gel process etc. to assemble atoms into more complex nanostructures **[6, 10]**. Physical and chemical methods require multi-step processing and might prove toxic to the environment. To circumvent the side effects associated with these methods, researchers are now shifting towards greener and safer techniques of nanoparticle synthesis. Biogenic synthesis of nanoparticles, a bottom up approach, can be achieved using various types of biological entities, such as plant extracts, microbial cell filtrate and isolated biomolecules such as peptides, carbohydrates and lipids. These biological entities and biomolecules not only act as efficient reducing agents but also serve as capping agents and provide stability to the suspension **[11-15]**. A wide array of phytochemicals are present in plant extracts, which not only reduce the metal salt into nanoparticles but also get adsorbed onto the surface of newly synthesized nanoparticles, providing stability in aqueous suspensions **[16]**. However, complex composition of plant extracts makes it difficult to elucidate the exact mechanism of reduction. **Table 1** lists various aspects of methods used for the synthesis of nanoparticles.

Table 1. Comparison of various methods employed for the synthesis of nanoparticles.

	Physical methods	**Chemical methods**	**Biological methods**
Approach	Top-down	Bottom-up	Bottom-up
Method	Mechanical and physical processes	Chemical assembly of atoms and molecules	Reduction of metal salts by biological entities
Process	Multi step	Multi step	Single step
Energy requirements	High	Moderate	Low
Nature	Toxic	Toxic	Non-toxic
Cost	High	High	Low
Ease of performance	Tedious	Tedious	Easy
Infrastructure	Specialized	Specialized	Common

Silver nanoparticles (AgNPs) have been shown to possess better antimicrobial potential as compared to the ionic form of the metal, making them one of the most popular metal nanoparticles to be used in antimicrobial applications **[17, 18]**. AgNPs are found to be active against as much as 650 types of pathogens including bacteria, fungi, yeasts, viruses etc. Not only do they show an excellent and rapid antibacterial activity, they also possess good antifungal potential against spore producing fungal pathogens and can also help fight against the problem of antibiotic resistance development **[17, 19, 20]**.

Elettaria cardamomum, also known as 'Elaichi', is an important member of household spices in India, best known for its aromatic and medicinal properties. In the present study, we report synthesis of silver nanoparticles using leaf extract of *Elettaria cardamomum.* Synthesis conditions were optimized for maximal synthesis and furthermore, antifungal potential of resultant AgNPs was evaluated for their efficacy against phytopathogens. *Elettaria* seed berry has numerous applications in everyday food items and are quite expensive and precious. In this paper, we are reporting utility of its leaves in place of seed for AgNP synthesis making the process more economic and ecofriendly. This is, to the best of our knowledge, the first report employing *Elettaria* leaf extract for AgNP synthesis and we, hereby, report an easy and eco-friendly method of AgNP synthesis.

Experimental

Materials

Silver nitrate (99.99% trace metals basis) was procured from Sigma-Aldrich Chemicals Pvt Ltd., Bangalore, India. Ketoconazole (minimum assay 98%), Potato Dextrose Agar (PDA) and Potato Dextrose Broth (PDB) were procured from HiMedia Laboratories Pvt. Ltd., Mumbai, India. Other chemicals were procured in analytical grade from local suppliers.

Leaves of *Elettaria cardamomum* plants were collected from the campus nursery of Deenbandhu Chhotu Ram University of Science and Technology, Murthal. Pure cultures of fungal phytopathogens, namely *Alternaria alternata* (ITCC 6531), *Aspergillus niger* (ITCC 7122), *Botrytis cinerea* (ITCC 6192), *Fusarium oxysporum* (ITCC 55) and *Penicillium expansum* (ITCC 6755) were procured from Indian Type Culture Collection, Indian Agricultural Research Institute, New Delhi.

Preparation of Elettaria leaf extract

Fresh leaves of *Elettaria* plants leaves were washed under running water first and then with distilled water several times to remove soil, dirt and any foreign particles. The leaves were cut into small pieces and boiled in 150 mL of double distilled water. Heating was stopped when the leaves lost their natural green colour and the solution turned yellowish brown in colour. Resultant solution was cooled and filtered using Whatman No.1 filter paper for further use. Fresh extract was prepared for every cycle of nanoparticle synthesis.

Synthesis of silver nanoparticles

Silver nitrate ($AgNO_3$) was used as a precursor for the biosynthesis of silver nanoparticle suspension. 1 mM solution of $AgNO_3$ was prepared with continuous stirring for 3-4 h using a magnetic stirrer at room temperature. To 45 mL of this solution, 5 mL of leaf extract was added, stirred well and the resultant solution was then left undisturbed at room temperature. A colour change from white to yellowish brown confirmed the synthesis of AgNPs. For purification, nanoparticles were centrifuged at 15000 rpm for 15 min, washed with ethanol twice and re-suspended in sterile de-ionized water.

Optimization of synthesis parameters

UV-Visible spectroscopy of the nanoparticle suspension was performed at different intervals of time viz., 30 min, 1 h, 2 h, 3 h and 4 h using UV-Vis Spectrophotometer UV-3092 from Labindia Analytical Instruments Pvt. Ltd. Synthesis parameters namely, metal ion concentration, leaf extract concentration, pH and temperature, are known to affect the biogenic synthesis of nanoparticles. These parameters were analyzed for optimum synthesis of nanoparticles. Metal ion concentrations were maintained at 0.5, 1, 2, 3, 4 and 5 mM. The results were noted after 24 h of incubation. All other parameters were kept constant during the reaction. Varying ratio of leaf extract and silver nitrate were also analyzed viz., 1:9, 2:8, 3:7, 4:6 and 5:5. Effect of pH on the synthesis of nanoparticles was investigated by maintaining pH of silver nitrate and extract mixture at 7, 9, 11 and 13, using 0.1 N HCl or 0.1 N NaOH. Leaf extract and silver nitrate were mixed in the ratio of 1:9 and incubated at different temperatures viz., 15, 25, 35, 45, 55, 65 and 75 °C for 24 h to analyze the effect of temperature on synthesis. Also, effect of room temperature storage on silver nanoparticles was observed in purified and raw form after 1 month and later. Spectrum scans were performed in the wavelength range of 200-700 nm and the spectra were re-plotted using OriginPro 8.

Fourier transform infrared (FT-IR) spectroscopy

In order to identify various phyto-chemical constituents in leaf extract and to ascertain the role they play in the reduction and stabilization of nanoparticle suspension, Fourier transform infrared (FT-IR) spectroscopy was performed. FT-IR spectrum for purified liquid AgNP suspension was obtained using Perkin Elmer FT-IR Spectrophotometer Frontier using Attenuated Total Reflectance (ATR) accessory in the range of 4000-500cm^{-1}.

X- ray diffraction (XRD)

For XRD, AgNPs were centrifuged at 15000 rpm for 15 min and the resultant pellet was left to dry onto a clean glass surface at 45°C. Dried sample was then collected, powdered and used for XRD analysis. XRD scan was performed using Ultima IV (Rigaku, Japan) with X-ray wavelength of 1.5406 Å in the 2θ range of 20-70 degrees. X-ray scan was performed in $2\theta/\theta$ continuous mode at 2 degrees per min, with a step size of 0.02. Tube voltage and tube current were maintained at 40 kV and 40 mA, respectively, with a divergence slit length of 10 mm.

Dynamic Light Scattering (DLS)

DLS of purified AgNP suspension was performed using Zetasizer Nano (DLS, Malvern Instruments, Worcestershire, UK). Hydrodynamic diameter and polydispersity index were measured as a function of time. The instrument is outfitted with a He/Ne red laser with a wavelength of 633 nm and detector was fixed at an angle of 173°. This optic arrangement maximizes scattered light detection and provides high sensitivity for nanoparticle size measurement. The study was performed at 25 °C with a count rate of 364.1 kcps and measurements were noted as function of time. Refractive indices of AgNPs and dispersant (water) are 1.59 and 1.33 respectively.

Transmission Electron Microscopy (TEM)

For TEM, AgNP sample was diluted 2 fold to yield slightly turbid suspension and sonicated using Sonomatic 375 by Langford Ultrasonics for 10 min. A drop of this suspension was then placed onto a copper grid, allowed to dry and loaded on a specimen holder. TEM observations were then performed using Morgagni 268D, FEI Electron Optics (USA) at an accelerating voltage of 200 kV to ascertain particle morphology and size. Results were visualized using Olympus siViewer.

Antifungal analysis of silver nanoparticles

Antifungal activity of silver nanoparticles was examined using agar well diffusion method. All the fungal strains were maintained on PDA at 28 °C and 5 day old cultures were used for antifungal analysis. 3-4 mL of sterile normal saline was poured onto the fungal lawns and conidia were collected by gentle scraping. 100 µL of this liquid spore suspension was evenly spread plated onto fresh PDA plates and two wells, 7 mm in diameter, were punched with a sterile metal borer. 50 µL of AgNP suspension was added as test solution and 10 µL of 2% ketoconazole was used as control. The plates were then incubated in upright position for 2-3 days at 25 ºC.

Minimum inhibitory concentration (MIC) of prepared AgNPs was calculated using broth microdilution method. For adjusting the spore count to 1×10^5 c.f.u./mL, OD_{530} value of fungal suspensions obtained was adjusted in the range of 0.05-0.1 and viability was confirmed by plating on solid media. These diluted suspensions were used as inoculums for microdilution assays **[21]**. For microdilution assay, 100 µL of sterile potato dextrose broth was added into the wells of a sterile microtiter plate. 100 µL of AgNP suspension (256 µg/mL) was added in first well and diluted two folds in subsequent wells. The wells were then inoculated with 5 µL of previously diluted conidia and incubated at 28 °C for 72 h. Lowest AgNP concentration that gave no visible fungal growth after 72 h was recorded as the MIC value.

Results and discussion

Addition of leaf extract resulted in visible colour change from transparent to yellowish brown, which could be taken as the first indication for synthesis of AgNPs in solution. This colour change appears as a result of surface plasmon resonance exhibited by the resultant nanoparticle suspension **[22]**. Silver nanoparticles are known to show strong absorption in UV-Visible spectrum at around 400 nm **[23]**. Absorption peaks at 420 nm using *Ceratonia siliqua* leaf extract **[22]**, 440 nm using *Terminalia chebula* fruit extract **[24]**, 445 nm and 460 nm using *Elettaria cardamomum* seed extract have been reported **[25, 26]**.

Optimization

UV-Visible spectrum for silver nanoparticles was noted at increasing time intervals. Increase in absorbance was observed with increase in time **(Fig. 1(a))**, which could be attributed to increasing concentration of nanoparticles with respect to time **[27]**. To access the stability of nanoparticle suspension, they were maintained in pure form after washing twice with ethanol to remove remnant of plant extract and unused silver nitrate and also in their as-formed state without any washing or purification. Nanoparticles in purified form retained their colloidal state and exhibited a sharp peak after 4 months of storage at room temperature **(Fig. 1(b))**. On the other hand, when kept in as-formed state, they lost their colloidal state and did not give characteristic peak.

Different concentrations of silver nitrate were used for optimization of biosynthesis. When the concentration was increased from 0.5 mM to 1 mM, increase in absorbance was observed and an intense peak was observed at 434 nm. However, further increase in concentration led to decrease in absorbance of the suspension, eventually leading to loss of peak **(Fig. 1(c))**. Results obtained were found to be in accordance to those reported by Vanaja et al. **[28]**. They have reported that

increasing the concentration of silver nitrate leads to the formation of larger and aggregated nanoparticles which could be observed as broadening of spectral peaks. Hence, 1 mM silver nitrate is reported as optimum for synthesis using *Elettaria* leaf extract.

Concentration of leaf extract is also known to affect biogenic synthesis of nanoparticles. Different ratios of extract and silver nitrate were tested. Leaf extract was added as 1, 2, 3, 4 and 5 mL in total 10 mL of reaction mixture. It was observed that the concentration ratio 1:9 gave an intense and sharp peak at 434 nm. When ratio of leaf extract was increased in the reaction mixture, significant peak broadening was observed accompanied by decrease in absorbance **(Fig. 1(d))**. Iravani and Zolfaghari have stated that increasing the quantity of *P. elderica* bark extract led to increase in absorbance of nanoparticle suspension. They have employed increasing extract volumes (1, 2, 4, and 6 mL) in 50 mL of silver nitrate **[27]**. Concentration ratio 1:9 in current study corresponds to approximately 5.6 mL of extract in 50 mL of silver nitrate and diminishing effects were observed upon further increasing extract volume in the reaction, which have not been covered by Iravani and Zolfaghari.

pH is one among various important factors that are known to affect the size of nanoparticles. Synthesis was performed while maintaining the reaction mixture at different pH values, viz., 7, 9, 11 and 13. When the reaction mixture was shifting to basic pH by addition of NaOH, an accelerated rate of reaction was observed. While colour change at neutral pH took about 3 h to appear distinctly, the same was evident within minutes of adding NaOH to the reaction mixture. Moreover, at basic pH, considerable increase in absorbance was observed, accompanied by narrowing of peak and shift of λ_{max} towards smaller wavelength, from 430 nm (pH 7) to 408 nm (pH 13) **(Fig. 1(e))**. It is reported that shift in surface plasmon resonance comes from change in size of nanoparticles and shift towards smaller wavelength further indicates that size of nanoparticles has reduced **[29]**. Thus, increasing the pH led to synthesis of smaller nanoparticles with a narrow range of size distribution. Similar trends have also been reported while synthesizing AgNPs using *Achyranthes aspera* leaf extract, where increasing the pH of reaction mixture, increased the rate of nanoparticle formation and intensity of the peak. Also, peak sharpening and λ_{max} shift indicated the synthesis of small sized monodispersed nanoparticles **[30]**.

To study the effect of temperature on synthesis of nanoparticles, reaction mixture was incubated at different temperatures for 24 h and results were noted in form of UV-Vis absorption spectra. It was observed that increasing the temperature from 15 °C to 75 °C led to increase in absorbance of the resultant suspension. At lower temperatures, significantly broad and less intense peaks were observed signifying inefficient synthesis of AgNPs. As the temperature was increased, a consistent increase in absorption and sharpening of peaks was noted. Shift of λ_{max} towards smaller wavelength was also observed and absorption peak shifted from 427nm at 35°C

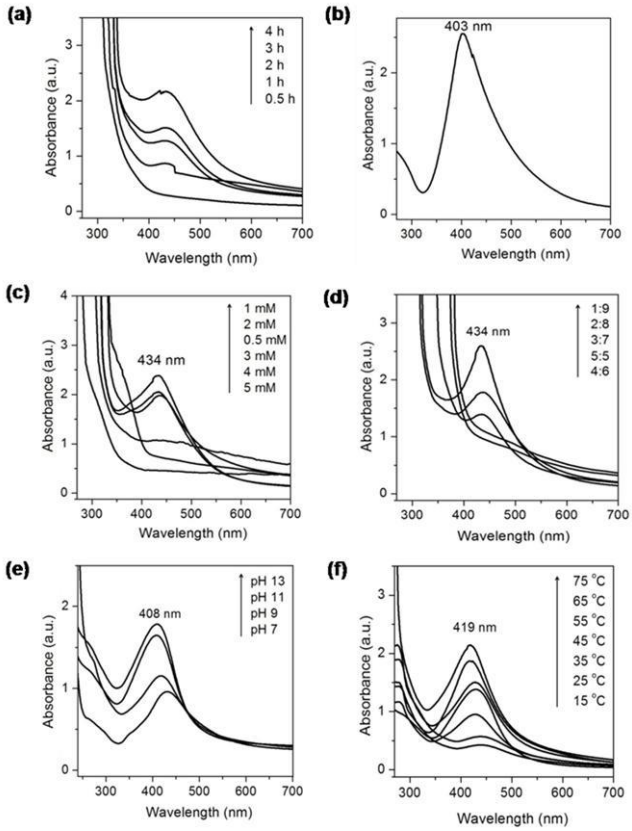

Fig. 1. (a) UV-Visible spectrum of AgNPs at increasing time intervals, (b) absorption spectra after 4 months of storage, (c) effect of metal ion concentration, (d) effect of extract: $AgNO_3$ ratio, (e) effect of pH, (f) effect of temperature

to 419 nm at 75 °C. This could again be attributed to decrease in the size of resultant nanoparticles **(Fig. 1(f))**. Similar effects were reported by Song and Kim and by Dwivedi and Gopal **[31, 32]**. Song and Kim further hypothesized that reduction in particle size with increasing temperature could be due to the fact that increasing the temperature led to an increase in rate of reaction consuming most of silver ions at a faster pace, thereby preventing secondary reduction process on these nuclei. Hence, increasing the temperature of the reaction mixture not only increased the concentration of silver nanoparticles performed but also reduced their size.

Characterization

To ascertain the functionalization of AgNPs, FT-IR was performed, the results of which are shown in **Fig. 2(a)**. Peaks were observed at 3320.33, 2900.54, 2111.29, 1636.11, 1472.01, 1263.13 and 618.20 cm^{-1}. The broad peak at 3320.33 cm-1 indicates the subsistence of H bonded –OH group stretch and is also indicative of $–NH_2$ group stretching. 2900.54 and 2111.29 correspond to stretching vibrations of CH_2 and CH_3 groups and C≡C stretch of alkynes, respectively. The sharp peak observed at 1636.11 could be accredited to stretching vibrations of C=C, C=O groups of alkenes and peptide linkages in amides. The peaks at 1472.01 and 1263.13 might be due to –NH amine stretch vibrations in protein amide linkages and C-H wag ($-CH_2X$) of alkyl halides, respectively.

Lastly, the peak at 618.20 corresponds to C-H bend of alkynes **[22, 25, 33-35]**. The data signifies –OH group, –NH group and C=O group as the main effectors for the reduction and stabilization of silver nanoparticles which in turn points towards the fact that protein component of the leaf extract supposedly play crucial role in nanoparticles synthesis. This is, however, supported by reports **[22, 36]** which have depicted the role of protein part of the plant extracts for reduction and capping of nanoparticles. Carbonyl groups, in particular bind strongly with metal, act as a stabilizing agent and maintain the colloidal state of nanoparticles **[22]**.

XRD analysis was performed to ascertain crystalline nature of synthesized silver nanoparticles **(Fig. 2(b))**. X-ray diffraction pattern showed intense peaks at 2θ values of 38.26°, 44.44° and 64.66° which were in accordance to those reported in the JCPDS file for Silver: 04-0783. XRD data analysis and peak indexing was performed as explained by Theivasanthi and Alagar **[37]** and it was concluded that the above stated 2θ values correspond to (111), (200) and (220) planes of Bragg's reflections for FCC structures **(Table 2)**. X-ray diffraction results clearly stated that synthesized AgNPs were crystalline in nature. A few intense yet unidentified peaks were also present which could have resulted from some biomolecules involved in nanoparticle synthesis.

Calculation of interplanar *d*-spacing was performed based on Bragg's Law, as presented below:

$$2d \sin\theta = n\lambda$$

where, $n = 1$, θ is angle of diffraction and λ is wavelength of X-rays used (0.154 nm) **(Table 2)**. Peak indexing based on the resultant *d* values yielded similar results as observed by 2θ indexing (not shown).

Table 2. XRD Peak Indexing and *d*-spacing.

Peak 2θ	sin θ	1000 × $\sin^2\theta$	1000 × $\sin^2\theta$/ 35	*hkl*	$d = \lambda / 2\sin\theta$ (Å)	*d* (nm)
38.26	0.328	108	3	111	2.3484	0.23484
44.44	0.378	143	4	200	2.0378	0.20378
64.66	0.535	286	8	220	1.4398	0.14398

Finally, particle size (*D*) calculation was performed using Debye-Scherrer formula, as stated below:

$$D = 0.9\lambda / \beta \cos\theta$$

where β= FWHM (Full Width at Half Maximum) and was calculated by Gaussian fitting of the diffraction peaks using OriginPro 8.0. Particle size as deciphered from the intense (111) peak is 29.96 nm **(Table 3)**.

Table 3. Particle size calculation.

Peak 2θ	θ	FWHM (deg)	FWHM (rad)	*D* (nm)
38.26	19.13	0.28063	0.004897	29.96
44.44	22.22	0.57269	0.00999	14.99
64.66	32.33	0.43085	0.00752	21.81

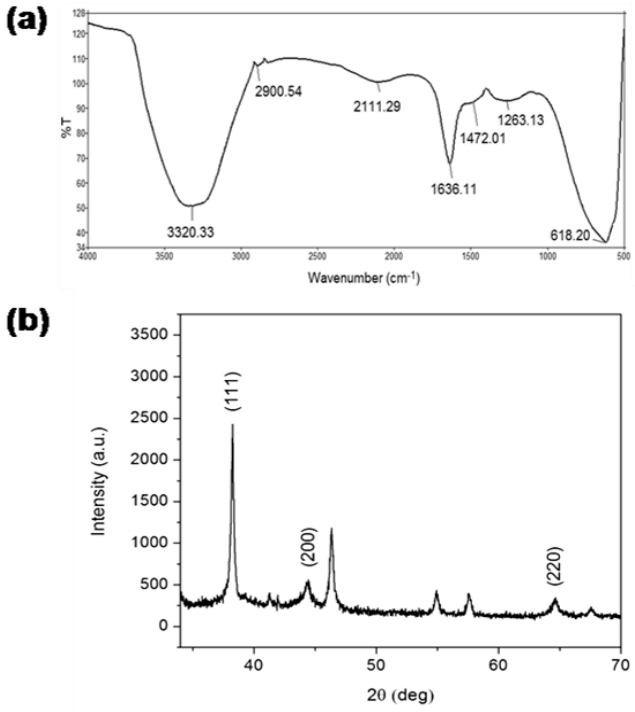

Fig. 2. (a) FT-IR spectrum, (b) X-ray diffraction pattern for silver nanoparticles.

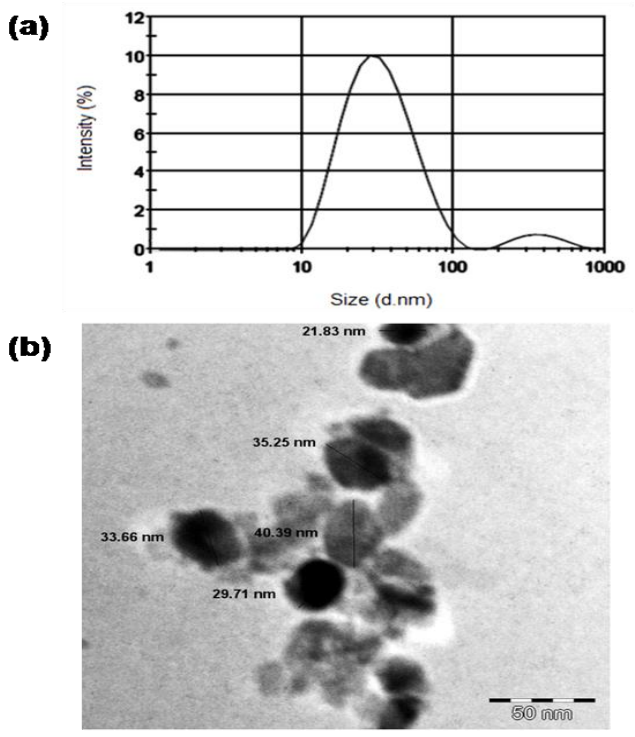

Fig. 3. (a) DLS analysis, (b) TEM image of silver nanoparticles.

DLS has become one of the most valued techniques for performing nanoparticle size calculation studies. DLS gave an average hydrodynamic diameter of 32.12 nm which is slightly higher than that calculated from the XRD data and may be due to the capping of biomolecules onto the surface of the nanoparticles **(Fig. 3(a))**.

Polydispersity index of 0.316 further specifies monodisperse nature of the AgNP suspension and absence of aggregation. TEM analysis of washed and purified silver nanoparticles, after 24-36 h of synthesis, showed irregularly spherical nanoparticles with a size range of 5- 80 nm **(Fig. 3(b))**.

Antifungal activity of AgNPs

AgNPs were investigated for their antifungal activity against five fungal phytopathogens. In general, nanoparticles exert their antimicrobial action by a number of mechanisms, complete elucidation of which has not yet been achieved. Researchers have implicated the role of various effector mechanisms such as membrane disintegration, DNA and protein damage, reactive oxygen species etc. in nanoparticle induced cell deaths. Silver nanoparticle mediated membrane damage is a three step process: (1) interaction of nanoparticles with the cell membrane; (2) accumulation into the membrane and penetration; and (3) disruption of membrane by the formation of pits. Membrane damage adversely affects the electrolyte balances in and out of the cell, eventually leading to cell death **[38-40]**. Release of silver ions play another important role in silver nanoparticle induced cell deaths. Silver ions inactivate cellular proteins and enzymes and initiate the release of reactive oxygen species, inhibiting essential metabolic reactions **[41, 42]**. Furthermore, silver ions interact with DNA and RNA molecules, induce DNA damage and hamper cell division **[43-45]**.

The antifungal activity of AgNPs was initially tested using agar well diffusion method. Varying degrees of inhibition were observed for all the fungi (not shown). MIC values of AgNPs for all the test fungi were then determined. Lowest MIC value of AgNPs was observed for *A. niger* (8 µg/mL), followed by *A. alternata*, *B. cinerea* and *F. oxysporum* which showed inhibition at 32 µg/mL. Highest MIC value of AgNPs was recorded for *P. expansum* which was found to be 64 µg/mL. The results signified strong antifungal potential of biosynthesized AgNPs.

Conclusion

The present study reports a simple and eco friendly approach for the synthesis of silver nanoparticles. Various reports are available for nanoparticle synthesis using *Elettaria* seeds but this is apparently the first report employing leaf extract of *Elettaria* for nanoparticle synthesis. Colour change of silver nitrate post addition of leaf extract is primary indication of nanoparticle synthesis which was further confirmed using UV- Visible spectroscopy, XRD, DLS and TEM. Irregularly spherical nanoparticles with a size range of 5-80 nm and average particle size of 29.96 nm were obtained. FTIR analysis implements the supposed role of plant proteins in the reduction and stabilization of nanoparticles. However, work still needs to be done to identify the actual causative agent. The synthesized nanoparticles showed good antifungal activity against all the tested fungal phytopathogens and could serve as potential antifungal agents.

Acknowledgements

The author Pragati Jamdagni is thankful to Assured Opportunity for Research Careers (AORC), Department of Science and Technology (DST), Ministry of Science and Technology, New Delhi for awarding INSPIRE fellowship. All the authors are thankful to Sophisticated Analytical Instrument Facility (SAIF), AIIMS for providing TEM facility and Indian Agricultural Research Institute (IARI) for supply of fungal cultures.

Author's contributions

Conceived the plan: PJ, JSR; Performed the expeirments: PJ, PK; Data analysis: PJ, PK; Wrote the paper: PJ, PK, JSR. Authors have no competing financial interests.

References

1. Feynman, R.P. *Eng. Sci*. **1960**, *23*, 22.
2. Tiwari, A. *Adv. Mater. Lett*. **2012**, *3*, 1.
3. El-Nour, K.M.M.A.; Eftaiha, A.; Al-Warthan, A.; Ammar, R.A.A. *Arabian J. Chem.* **2010**, *3*, 135.
4. Syed, M. A. *Biosens. Bioelectron.* **2014**, *51*, 391.
5. Alex, S.; Tiwari, A. *J. Nanosci. Nanotechnol*. **2015**, *15*, 1869.
6. Chauhan, P.; Mishra, M.; Gupta, D. Potential Application of Nanoparticles as Antipathogens, In Advanced Materials for Agriculture, Food, and Environmental Safety; Tiwari, A.; Syväjärvi, M. (Eds.); John Wiley & Sons: USA, **2014**, pp. 333-368.
7. Mishra, S.; Singh, H.B. *Appl. Microbiol. Biotechnol.* **2015**, *99*, 1097.
8. Stark, W.J.; Stoessel, P.R.; Wohlleben, W.; Hafner, A. *Chem. Soc. Rev*. **2015**, *44*, 5793.
9. Jamdagni, P.; Khatri, P.; Rana, J.S. *Int. Nano Lett.* **2016**, *6*, 139.
10. Pacioni, N.L.; Borsarelli , C.D.; Rey, V.; Veglia, A.V. Synthetic Routes for the Preparation of Silver Nanoparticles, In Silver Nanoparticle Applications; Alarcon, E.I.; Griffith, M.; Udekwu, K.I. (Eds.); Springer: Heidelberg, **2015**, pp. 13–46.
11. Sharma, T.K.; Chopra, A.; Sapra, M.; Kumawat, D.; Patil, S.D.; Pathania, R.; Navani, N.K. *Int. J. Green Nanotechnol*. **2012**, *4*, 1.
12. Akhtar, M.S.; Panwar, J.; Yun, Y-S. *ACS Sustainable Chem. Eng*. **2013**, *1*, 591.
13. Jamdagni, P.; Khatri, P.; Rana, J.S. *J. King Saud Univ., Sci*. **2016**. http://dx.doi.org/10.1016/j.jksus.2016.10.002
14. Jeevanandam, J.; Chan, Y.S.; Danquah, M.K. *ChemBioEng Rev.* **2016**, *3*, 55.
15. Singh, P.; Kim, Y-J.; Zhang, D.; Yang, D-C. *Trends Biotechnol.* **2016**, *34*, 588.
16. Shanker, U.; Jassal, V.; Rani, M.; Kaith, B.S. *Int. J. Environ. Anal. Chem*. **2016**, 96, 801.
17. Jo, Y.K.; Kim, B.H.; Jung G. *Plant Dis*. **2009**, *93*, 1037.
18. Zinjarde, S.S. *Chron. Young Sci.* **2012**, *3*, 74.
19. Shahrokh, S.; Emtiazi, G. *Eur. J. Biol. Sci.* **2009**, *1*, 28.
20. Rai, M.; Yadav, A.; Gade, A. *Biotechnol. Adv*. **2009**, *27*, 76.
21. Silveira, C.P.; Torres-Rodríguez, J.M.; Alvarado-Ramírez, E.; Murciano-Gonzalo, F.; Dolande, M.; Panizo, M.; Reviakina, V. *J. Med. Microbiol*. **2009**, *58*, 1607.
22. Awwad, A.M.; Salem, N.M.; Abdeen, A.O. *Int. J. Ind. Chem.* **2013**, *4*, 29.
23. Henglein, A. *Chem. Mater*. **1998**, *10*, 444.
24. Edison, T.J.I.; Sethuraman, M.G. *Process Biochemistry*, **2012**, *47*, 1351.
25. GnanaJobitha, G.; Annadurai, G.; Kannan, C. *Int. J. Pharma Sci. Res.* **2012**, *3*, 323.
26. Dhiman, J.; Kundu, V.; Kumar, S.; Kumar, R.; Chakarvarti, S.K. *Am. J. Mater. Sci. Technol*. **2014**, *3*, 13.
27. Iravani, S.; Zolfaghari, B. *BioMed. Res. Int*. **2013**, *2013*, 639725.
28. Vanaja, M.; Rajeshkumar, S.; Paulkumar, K.; GnanaJobitha, G.; Malarkodi, C.; Annadurai, G. *Adv. Appl. Sci. Res*. **2013**, *4*, 50.
29. Alqadi, M.K.; Noqtah, O.A.A.; Alzoubi, F.Y.; Alzouby, J.; Aljarrah, K. *Mater. Sci.-Pol*. **2014**, *32*, 107.

30. Amaladhas, T.P.; Usha, M.; Naveen, S. *Adv. Mater. Lett.* **2013**, *4*, 779.
31. Song, J.Y.; Kim, B.S. *Bioprocess Biosyst. Eng*. **2009**, *32*, 79.
32. Dwivedi, A.D.; Gopal, K. *Colloids Surf., A.* **2010**, *369*, 27
33. Rastogi, L.; Arunachalam, J. *Mater. Chem. Phys*. **2011**, *129*, 558.
34. Parida, U.K.; Biswal, S.K.; Bindhani, B.K.; Nayak, P.L. *World Appl. Sci. J*. **2013**, *28*, 962.
35. Spectroscopy Tutorial. Department of Chemistry and Biochemistry, University of Colorado, Boulder. http://orgchem.colorado.edu/Spectroscopy/specttutor/irchart.html. Accessed Dec 18, 2015.
36. Shankar, S. S.; Ahmad, A.; Sastry, M. *Biotechnol. Prog*. **2003**, *19*, 1627.
37. Theivasanthi,T.; Alagar, M. *Nano Biomed. Eng.* **2012**, *4*, 58.
38. Sondi, I.; Salopek-Sondi, B. *J. Colloid Interface Sci*. **2004**, *275*, 177.
39. Iavicoli, I.; Fontana, L.; Leso, V.; Bergamaschi, A. *Int. J. Mol. Sci.* **2013**, *14*, 16732.
40. Yun, H.; Kim, J.D.; Choi, H.C.; Lee, C.W. *Bull. Korean Chem. Soc*. **2013**, *34*, 3261.
41. Matsumura, Y.; Yoshikata, K.; Kunisaki, S.; Tsuchido, T. *Appl. Environ. Microbiol*. **2003**, *69*, 4278.
42. Egger, S.; Lehmann, R.P.; Height, M.J.; Loessner, M.J.; Schuppler, M. *Appl. Environ. Microbiol*. **2009**, *75*, 2973.
43. Feng, Q.L.; Wu, J.; Chen, G.Q.; Cui, F.Z.; Kim, T.N.; Kim, J.O. *J. Biomed. Mater. Res.* **2000**, *52*, 662.
44. Lansdown, A.B.G. *Journal of Wound Care*. **2002**, *11*, 125.
45. Castellano, J.J.; Shafii, S.M.; Ko, F.; Donate, G.; Wright, T.E.; Mannari, R.J.; Payne, W.G.; Smith, D.J.; Robson, M.C. *International Wound Journal*. **2007**, *4*, 114.

